PROCEEDINGS OF SCIENCE

# Electroweak corrections to hadronic Z + 2 jets production

**Ansgar Denner***
*Universität Würzburg*
*E-mail:* denner@physik.uni-wuerzburg.de

**Lars Hofer**
*IFAE, Universitat Autònoma de Barcelona*
*E-mail:* lhofer@ifae.es

**Andreas Scharf**
*Universität Würzburg*
*E-mail:* ascharf@physik.uni-wuerzburg.de

**Sandro Uccirati**
*Università di Torino*
*E-mail:* uccirati@to.infn.it

Using the amplitude generator RECOLA and the tensor-integral library COLLIER we have calculated the electroweak radiative corrections to the production of a Z boson in association with two jets at the LHC including the leptonic decay of the Z boson. The electroweak corrections turn out to be at the level of $-3\%$ for inclusive cross sections but reach several tens of percent in high-energy tails of distributions. The large corrections result from the virtual one-loop amplitude.

*Loops and Legs in Quantum Field Theory*
*27 April 2014 - 02 May 2014*
*Weimar, Germany*

*Speaker.

 

PoS(LL2014)058

## 1. Introduction

With the discovery of the Higgs boson at the LHC the last missing particle of the Standard Model (SM) has been found. On the other hand, with the exception of neutrino oscillations, no convincing evidence for physics beyond the standard model has emerged so far in particle-physics experiments. Lacking signals for new physics we are bound to study SM processes precisely in order to reveal possible small deviations from the SM. To this end higher-order perturbative corrections have to be taken into account in the theoretical predictions. The inclusion of QCD corrections, which are typically of the order of several ten per cent or more, has become more or less standard by now. However, also electroweak (EW) corrections must be included in an adequate theoretical description of phenomenologically interesting processes at the LHC. While they are often (but not always) small for inclusive observables, they are typically strongly enhanced in high-energy tails of distributions or near resonances and usually reach several ten per cent for energy scales in the TeV region.

By now, the automation of the calculation of next-to-leading order (NLO) QCD corrections is more or less completed. Different groups have developed software packages [1, 2, 3, 4, 5, 6, 7, 8, 9] and applied them to the evaluation of complicated hadronic processes. Electroweak corrections on the other hand have only been considered by few groups. We have constructed RECOLA, a generator of one-loop (and tree) amplitudes in the full SM [10, 11] including in particular EW corrections. In this approach, the coefficients of the tensor integrals are calculated numerically from recursion relations [12]. The tensor integrals on the other hand are evaluated with COLLIER, a Complex One-Loop LIbrary with Extended Regularisations [13, 14, 15, 16], which provides one-loop scalar and tensor integrals for arbitrary scattering processes.

We have used RECOLA to calculate the EW corrections to the process $pp \to Z+2\,\text{jets} \to \ell^+\ell^- + 2\,\text{jets}$. This process has a large cross section and provides similar signatures as Higgs-boson production in vector-boson fusion. Thus, it can be used for stringent tests of the SM and the study of the systematics for the $H+2\,\text{jets}$ final state. The NLO QCD corrections to the QCD production of $Z+2\,\text{jets}$ have been investigated in Ref. [17], while NLO QCD corrections to the EW $Z+2\,\text{jets}$ production have been studied in Ref. [18]. EW corrections in the Sudakov approximation have been considered in Ref. [19]. Here we summarise the calculation of the complete EW corrections of $\mathcal{O}(\alpha_s^2\alpha^3)$.

## 2. $Z+2$ jets production at the LHC

We study the production of a lepton pair $\ell^+\ell^-$ in association with 2 hard jets in proton–proton collisions, including diagrams with a resonant Z boson as well as all irreducible background diagrams.

### 2.1 Leading-order contributions

At leading order (LO), we get contributions from the partonic subprocesses

$$q_i\,\mathrm{g} \to q_i\,\mathrm{g}\,\ell^+\ell^-, \tag{2.1}$$

$$q_i\,\bar{q}_i \to q_j\,\bar{q}_j\,\ell^+\ell^-, \quad q_i,q_j = \mathrm{u},\mathrm{c},\mathrm{d},\mathrm{s},\mathrm{b}, \tag{2.2}$$

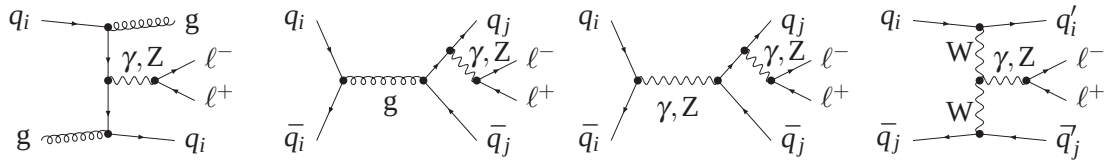


**Figure 1:** From left to right: Sample tree diagrams for the QCD contributions to $q_i\,\mathrm{g} \to q_i\,\mathrm{g}\,\ell^+\ell^-$ and $q_i\,\bar{q}_i \to q_j\,\bar{q}_j\,\ell^+\ell^-$, and the EW contributions to $q_i\,\bar{q}_i \to q_j\,\bar{q}_j\,\ell^+\ell^-$ and $q_i\,\bar{q}_j \to q_i'\,\bar{q}_j'\,\ell^+\ell^-$.

and all processes that result from these via crossing. While the mixed quark–gluon (gluonic) channels (2.1) contribute to the cross section exclusively at order $\mathcal{O}(\alpha_\mathrm{s}^2\alpha^2)$, the four-quark channels (2.2) involve LO diagrams of strong as well as of EW nature leading to contributions of order $\mathcal{O}(\alpha_\mathrm{s}^2\alpha^2)$, $\mathcal{O}(\alpha_\mathrm{s}\alpha^3)$, and $\mathcal{O}(\alpha^4)$. Representative Feynman diagrams are shown in Fig. 1. Photon-induced contributions are below 0.05% and have been omitted.

### 2.2 Setup of NLO calculation

A full NLO calculation of the cross section would contain contributions of orders $\mathcal{O}(\alpha_\mathrm{s}^3\alpha^2)$, $\mathcal{O}(\alpha_\mathrm{s}^2\alpha^3)$, $\mathcal{O}(\alpha_\mathrm{s}\alpha^4)$, and $\mathcal{O}(\alpha^5)$. We aim for the most important EW corrections and consider the contributions of $\mathcal{O}(\alpha_\mathrm{s}^2\alpha^3)$ which involve NLO EW corrections to the dominant LO contributions of $\mathcal{O}(\alpha_\mathrm{s}^2\alpha^2)$ and NLO QCD corrections to the LO interference contributions of $\mathcal{O}(\alpha_\mathrm{s}\alpha^3)$.

Resonant Z-boson propagators are treated by using the complex-mass scheme [20, 21, 22], i.e. we employ the complex masses

$$\mu_\mathrm{Z}^2 = M_\mathrm{Z}^2 - \mathrm{i}M_\mathrm{Z}\Gamma_\mathrm{Z}, \qquad \mu_\mathrm{W}^2 = M_\mathrm{W}^2 - \mathrm{i}M_\mathrm{W}\Gamma_\mathrm{W} \tag{2.3}$$

for the Z and W bosons throughout. Renormalisation is performed within the complex-mass scheme as described in Ref. [21].

We define the electromagnetic coupling constant $\alpha$ within the $G_\mu$ scheme, i.e. we use

$$\alpha_{G_\mu} = \frac{\sqrt{2}G_\mu M_\mathrm{W}^2}{\pi}\left(1 - \frac{M_\mathrm{W}^2}{M_\mathrm{Z}^2}\right). \tag{2.4}$$

Thus, higher-order effects of the renormalisation-group running from 0 to $M_\mathrm{W}^2$ are included in leading order. The counterterm corresponding to $\alpha_{G_\mu}$ inherits a correction term $\Delta r$ from the weak corrections to muon decay and the renormalisation of $\alpha$ becomes independent of light quark masses.

### 2.3 Virtual corrections

The virtual corrections contributing at $\mathcal{O}(\alpha_\mathrm{s}^2\alpha^3)$ involve $\mathcal{O}(1200)$ diagrams for a single gluonic channel, including 18 hexagons and 85 pentagons, and an almost comparable number of diagrams for a single typical four-quark channel. The most complicated topologies involve 6-point functions up to rank 4 (see Fig. 2 for sample diagrams). The virtual amplitude is calculated using the 't Hooft–Feynman gauge.

Since channels involving external bottom quarks contribute only at the per-cent level at leading order, they are neglected at NLO. In closed fermion loops the finite top-quark mass is fully included.

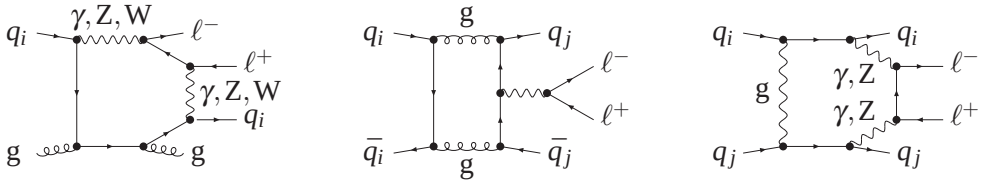


**Figure 2:** From left to right: Sample one-loop diagrams for the EW corrections to $q_i\,\mathrm{g} \to q_i\,\mathrm{g}\,\ell^+\ell^-$, the QCD corrections to $q_i\,\bar{q}_i \to q_j\,\bar{q}_j\,\ell^+\ell^-$, and the EW corrections to $q_i\,q_j \to q_i\,q_j\,\ell^+\ell^-$.

### 2.4 Real corrections

The real EW corrections of $\mathcal{O}(\alpha_s^2\alpha^3)$ consist of real photon emission from the LO QCD diagrams in all subprocesses (2.1), i.e. the processes

$$q_i\,\mathrm{g} \to q_i\,\mathrm{g}\,\ell^+\ell^-\,\gamma, \tag{2.5}$$

$$q_i\,\bar{q}_i \to q_j\,\bar{q}_j\,\ell^+\ell^-\,\gamma, \tag{2.6}$$

and from real gluon emission contributions in the interferences between LO QCD and EW diagrams, i.e. the processes

$$q_i\,\bar{q}_i \to q_j\,\bar{q}_j\,\ell^+\ell^-\,\mathrm{g}. \tag{2.7}$$

The amplitudes can be constructed exactly as for LO, but we only take into account contributions of $\mathcal{O}(\alpha_s^2\alpha^3)$. Crossing of a the gluon in (2.7) leads to the additional partonic channels

$$q_i\,\mathrm{g} \to q_j\,\bar{q}_j\,\ell^+\ell^-\,q_i. \tag{2.8}$$

We use dimensional regularisation for the IR divergences of soft or collinear photons and gluons and the Catani–Seymour dipole subtraction formalism [23] as formulated in Refs. [24, 25, 26], which we adapted to the case of dimensionally regularised photon emission.

The presence of gluons in the final state of the LO process (2.1) introduces additional IR singularities at NLO. In IR-safe observables quarks, and thus all QCD partons, have to be recombined with collinear photons. As a consequence, a soft gluon passes the selection cuts once it is recombined with a hard collinear photon, giving rise to a soft-gluon divergence. This kinematical situation corresponds to soft-gluon corrections to $\ell^+\ell^- + 1\,\mathrm{jet} + \gamma$ production and would be cancelled by the virtual QCD corrections to this process. Employing the strategy of Ref. [27] we eliminate this singularity by discarding events containing a jet consisting of a hard photon and a soft parton $a$ ($a = q_i, \bar{q}_i, \mathrm{g}$) where the photon–jet energy fraction $z_\gamma = E_\gamma/(E_\gamma + E_a)$ is above a threshold. Finally, we absorb the left-over singularities into contributions involving the quark–photon fragmentation function [28].

### 2.5 Implementation

All tree-level, one-loop and bremsstrahlung amplitudes have been generated with the amplitude generator RECOLA [10, 11]. The one-loop tensor integrals are obtained from the tensor-integral library COLLIER [16], that provides a fast and numerically stable calculation. For the phase-space integration we employ an in-house multi-channel Monte-Carlo generator [29].

Various cross-checks of the calculation have been performed based on conventional methods. For the checks we have used FEYNARTS 3.2 [30, 31], FORMCALC 3.1 [32] and POLE [33] for

| process class | $\sigma^{\rm LO}$ [fb] | $\sigma^{\rm LO}/\sigma^{\rm LO}_{\rm tot}$ [%] | $\sigma^{\rm NLO}_{\rm EW}$ [fb] | $\frac{\sigma^{\rm NLO}_{\rm EW}}{\sigma^{\rm LO}}-1$ [%] |
|---|---|---|---|---|
| $qg \to qg\ell^-\ell^+$<br>$\bar{q}g \to \bar{q}g\ell^-\ell^+$ | 34584(8) | 67.5 | 33751(9) | -2.41 |
| $q\bar{q} \to gg\ell^-\ell^+$ | 2713(1) | 5.3 | 2626(1) | -3.21 |
| $gg \to q\bar{q}\ell^-\ell^+$ | 3612(1) | 7.1 | 3556(1) | -1.55 |
| gluonic | 40910(8) | 79.9 | 39932(9) | -2.39 |
| four-quark | 10299(1) | 20.1 | 10033(1) | -2.58 |
| sum | 51209(8) | 100.0 | 49965(9) | -2.43 |
| bottom quarks | 4376(3) | 8.54 | | |

**Table 1:** LO cross section for $pp \to \ell^+\ell^- + 2\,\text{jets}$ at the 13 TeV LHC split into different contributions. The second column provides the LO cross section with integration error on the last digit in parentheses, the third column contains the relative contribution to the total cross section in per cent, the fourth column the NLO EW cross section, and the last column the relative EW corrections.

the generation, simplification and calculation of the Feynman amplitudes. The tensor integrals are evaluated by COLLIER, which includes a second independent implementation of all its building blocks. The phase-space integration is performed with the multi-channel generator LUSIFER [34].

### 2.6 Numerical results

We show some results for the LHC at 13 TeV using the input parameters of Ref. [10]. We employ the MSTW2008LO PDF set [35] and choose $\mu_{\rm F} = \mu_{\rm R} = M_{\rm Z}$ for the QCD factorisation and renormalisation scales.

Jets are formed with the anti-$k_{\rm T}$ algorithm [36] with separation parameter $R = 0.4$. Photons and leptons are included in the jet clustering in the sense that also photons and quark/gluons as well as leptons and photons are recombined according to the anti-$k_{\rm T}$ description with $R = 0.4$. The photon energy fraction $z_\gamma$ in a jet must be less than 0.7. We require two hard jets with

$$p_{\rm T,jet} > 30\,\text{GeV}, \qquad |y_{\rm jet}| < 4.5. \tag{2.9}$$

We then apply to the resulting two or three jets and the two charged leptons the cuts

$$\begin{aligned} p_{{\rm T},\ell} &> 20\,\text{GeV}, \qquad |y_\ell| < 2.5, \\ \Delta R_{\ell\ell} &> 0.2, \qquad \Delta R_{\ell\,\rm jet} > 0.5, \\ 66\,\text{GeV} &< M_{\ell\ell} < 116\,\text{GeV} \end{aligned} \tag{2.10}$$

for the transverse momenta $p_{\rm T}$, rapidities $y$, rapidity–azimuthal angle separation $\Delta R$, and invariant mass $M_{\ell\ell}$ of the lepton pair.

Results for the cross section in the set-up (2.9) and (2.10) are listed in Table 1. The total cross section is dominated by processes with external gluons, which amount to 80%, the largest contributions arising from the $qg$ initial state. The relative EW corrections are roughly $-2.5\%$ in this set-up and similar for all channels.

In Fig. 3 we show results for the differential cross section as a function of the transverse momentum of the lepton pair and the azimuthal angle between the two leptons for the cuts (2.9) and

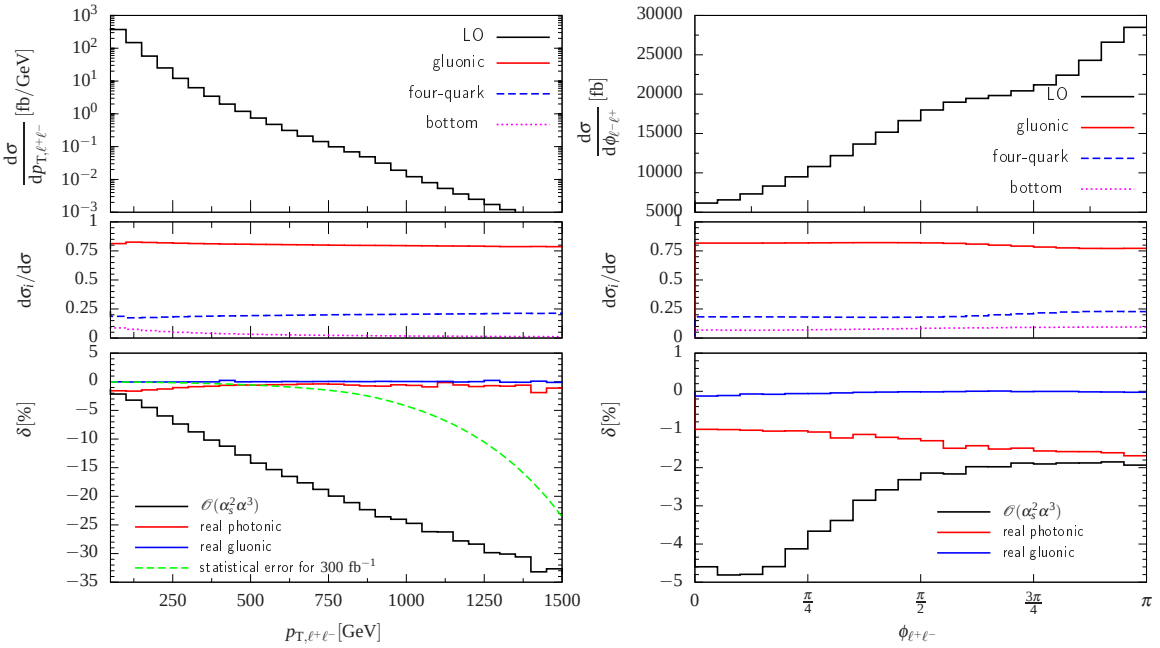


**Figure 3:** Distributions of the transverse momentum of the lepton pair $\ell^+\ell^-$ (left) and the azimuthal angle between the two leptons (right) at the 13 TeV LHC. The upper panels show the LO and the central panels the relative contributions of gluonic (red), four-quark (blue) and bottom (magenta, dashed) channels at LO. In the lower panels we show the total relative corrections (black) from $\mathcal{O}(\alpha_s^2\alpha^3)$ contributions, the included real photonic (red) and real gluonic (blue) corrections together with the statistical error (green, dashed) for 300 fb$^{-1}$.

(2.10). Both distributions are dominated by the gluon channels over the full considered kinematic range. This is in contrast to the transverse momentum distribution of the jets, which is dominated by the four-quark channels at high transverse momenta (see Ref. [37]). The contributions with external bottom quarks are always below 10% and become less important for large transverse momenta. The electroweak corrections to the $p_{T,\ell^+\ell^-}$ distribution reach about $-25\%$ for $p_{T,\ell^+\ell^-} \approx 1$ TeV. The (subtracted) real corrections from photon and gluon emission stay below 2% also for high $p_{T,\ell^+\ell^-}$. This indicates that the large negative EW corrections result from Sudakov logarithms in the virtual contributions. The relevance of the electroweak corrections can be seen by comparing with the statistical uncertainty depicted for an integrated luminosity of 300 fb$^{-1}$. The $\phi_{\ell^+\ell^-}$ distribution is distorted at the level of 3% by the electroweak corrections. Also this effect results mainly from the virtual corrections.

## 3. Conclusions

We have calculated the NLO corrections of order $\mathcal{O}(\alpha_s^2\alpha^3)$ to the production of $\ell^+\ell^- + 2$ jets at the LHC. These involve electroweak corrections to the LO QCD diagrams and QCD corrections to the interferences between LO QCD and EW diagrams. The results have been obtained with the amplitude generator RECOLA and the tensor-integral library COLLIER. The electroweak corrections turn out to be at the level of $-3\%$ for inclusive cross sections at 13 TeV. In the high-energy

tails of transverse-momentum distributions large EW corrections appear which can be attributed to EW Sudakov logarithms.

**Acknowledgements**

This work was supported in part by the Deutsche Forschungsgemeinschaft (DFG) under reference number DE 623/2-1. The work of L.H. was supported by the grant FPA2011-25948.

## References

[1] C. F. Berger, et al., Phys. Rev. D **78** (2008) 036003 [arXiv:0803.4180 [hep-ph]].

[2] W. T. Giele and G. Zanderighi, JHEP **0806** (2008) 038 [arXiv:0805.2152 [hep-ph]].

[3] A. Lazopoulos, arXiv:0812.2998 [hep-ph].

[4] W. Giele, Z. Kunszt and J. Winter, Nucl. Phys. B **840** (2010) 214 [arXiv:0911.1962 [hep-ph]].

[5] S. Badger, B. Biedermann and P. Uwer, Comput. Phys. Commun. **182** (2011) 1674 [arXiv:1011.2900 [hep-ph]].

[6] V. Hirschi, et al., JHEP **1105** (2011) 044 [arXiv:1103.0621 [hep-ph]].

[7] G. Bevilacqua, et al., Comput. Phys. Commun. **184** (2013) 986 [arXiv:1110.1499 [hep-ph]].

[8] G. Cullen, et al., Eur. Phys. J. C **72** (2012) 1889 [arXiv:1111.2034 [hep-ph]].

[9] F. Cascioli, P. Maierhöfer and S. Pozzorini, Phys. Rev. Lett. **108** (2012) 111601 [arXiv:1111.5206 [hep-ph]].

[10] S. Actis, et al., JHEP **1304** (2013) 037 [arXiv:1211.6316 [hep-ph]].

[11] S. Actis, A. Denner, L. Hofer, A. Scharf and S. Uccirati, these proceedings.

[12] A. van Hameren, JHEP **0907** (2009) 088 [arXiv:0905.1005 [hep-ph]].

[13] A. Denner and S. Dittmaier, Nucl. Phys. B **658** (2003) 175 [hep-ph/0212259].

[14] A. Denner and S. Dittmaier, Nucl. Phys. B **734** (2006) 62 [hep-ph/0509141].

[15] A. Denner and S. Dittmaier, Nucl. Phys. B **844** (2011) 199 [arXiv:1005.2076 [hep-ph]].

[16] A. Denner, S. Dittmaier and L. Hofer, these proceedings.

[17] J. M. Campbell and R. K. Ellis, Phys. Rev. D **65** (2002) 113007 [hep-ph/0202176];
J. M. Campbell, R. K. Ellis and D. L. Rainwater, Phys. Rev. D **68** (2003) 094021 [hep-ph/0308195].

[18] C. Oleari and D. Zeppenfeld, Phys. Rev. D **69** (2004) 093004 [hep-ph/0310156].

[19] M. Chiesa, et al., Phys. Rev. Lett. **111** (2013) 121801 [arXiv:1305.6837 [hep-ph]].

[20] A. Denner, S. Dittmaier, M. Roth and D. Wackeroth, Nucl. Phys. B **560** (1999) 33 [hep-ph/9904472].

[21] A. Denner, S. Dittmaier, M. Roth and L. H. Wieders, Nucl. Phys. B **724** (2005) 247 [Erratum-ibid. B **854** (2012) 504] [hep-ph/0505042].

[22] A. Denner and S. Dittmaier, Nucl. Phys. Proc. Suppl. **160** (2006) 22 [hep-ph/0605312].

[23] S. Catani and M. H. Seymour, Nucl. Phys. B **485** (1997) 291 [Erratum-ibid. B **510** (1998) 503] [hep-ph/9605323].

[24] Z. Nagy and Z. Trocsanyi, Phys. Rev. D **59** (1999) 014020 [Erratum-ibid. D **62** (2000) 099902] [hep-ph/9806317].

[25] Z. Nagy, Phys. Rev. D **68** (2003) 094002 [hep-ph/0307268].

[26] J. M. Campbell, R. K. Ellis and F. Tramontano, Phys. Rev. D **70** (2004) 094012 [hep-ph/0408158].

[27] A. Denner, S. Dittmaier, T. Gehrmann and C. Kurz, Nucl. Phys. **B836** (2010) 37 [arXiv:1003.0986 [hep-ph]].

[28] E. W. N. Glover and A. G. Morgan, Z. Phys. C **62** (1994) 311;
D. Buskulic *et al.* [ALEPH Collaboration], Z. Phys. C **69** (1996) 365.

[29] T. Motz, PhD thesis, Zürich 2011.

[30] T. Hahn, Comput. Phys. Commun. **140** (2001) 418 [hep-ph/0012260].

[31] T. Hahn and C. Schappacher, Comput. Phys. Commun. **143** (2002) 54 [hep-ph/0105349].

[32] T. Hahn and M. Pérez-Victoria, Comput. Phys. Commun. **118** (1999) 153 [hep-ph/9807565].

[33] E. Accomando, A. Denner and C. Meier, Eur. Phys. J. C **47** (2006) 125 [hep-ph/0509234].

[34] S. Dittmaier and M. Roth, Nucl. Phys. B **642** (2002) 307 [hep-ph/0206070].

[35] A. D. Martin *et al.*, Eur. Phys. J. C **63**, (2009) 189 [arXiv:0901.0002 [hep-ph]].

[36] M. Cacciari, G. P. Salam and G. Soyez, JHEP **0804** (2008) 063 [arXiv:0802.1189 [hep-ph]].

[37] A. Denner, L. Hofer, A. Scharf and S. Uccirati, PoS RADCOR **2013** (2014) 019 [arXiv:1311.5336 [hep-ph]].